



## Removal of methylene blue using polyacrylonitrile yarn waste/carboxylic group functionalized multiwall carbon nanotube nanofibrous composite

S. Swaminathan<sup>a,\*</sup>, N.M. Imayathamizhan<sup>a</sup>, A. Muthumanickam<sup>a</sup>, G. Baskar<sup>b</sup>

<sup>a</sup>Department of Textile Technology, Anna University, Chennai, India, email: swamychemdpi@gmail.com (S. Swaminathan), nmimayathamizhan@gmail.com (N.M. Imayathamizhan), pearlrubyruuby@gmail.com (A. Muthumanickam)

<sup>b</sup>Department of Biotechnology, St. Joseph's college of Engineering, Chennai, India, email: Basg2004@gmail.com (G. Baskar)

Received 8 September 2017; Accepted 4 March 2018

### ABSTRACT

Electrospun nanofibrous composites were prepared from polyacrylonitrile yarn waste (PAN) and carboxylic group functionalized multiwall carbon nanotubes (COOH-MCNT) with 0.5, 1.0 and 1.5% (w/w). The higher thermal stability of nanofibres was confirmed using Thermo Gravimetric Analysis (TGA). The presence of carboxyl group was confirmed by Fourier transform infrared (FT-IR) analysis. Scanning Electron Microscope (SEM) results confirmed the rough and irregular surface of nanofibres. The adsorption capacity of the PAN-COOH-MCNT nanofibrous composites were evaluated systematically with methylene blue (MB) as an adsorbate. The adsorption studies were conducted with various physical and chemical parameters such as contact time, solution pH and initial dye concentration. The nanofibrous composite was acquired the maximum amount of methylene blue dye removal under basic pH (10) at initial dye concentration of 30 mg/L. The pseudo second order kinetic model was found to be most fitted for the adsorption of methylene blue with higher R<sup>2</sup> value (0.993). The external diffusion model was adapted to understand the diffusion mechanism of adsorption. It was observed that the Freundlich and Scatchard isotherm models are more favourable for the adsorption of methylene blue. The prepared PAN/COOH-MCNT nanofibrous composite was a potential adsorbent for the removal of methylene blue dye.

*Keywords:* Polyacrylonitrile yarn waste; Functionalized multiwall carbon nanotube; Methylene blue; Adsorption isotherm; Kinetics

### 1. Introduction

The textile, feedstuffs, paper, leather, cosmetics industries, food producers and electroplating factories are used dyes for coloring the products [1] and it leads to discharge large amounts of dye-containing effluents. More than 100,000 commercial dyes are known with the annual production of  $7 \times 10^5$  tonnes per year [2,3]. Worldwide the total dye consumption in textile industry is more than 10,000 tonnes per year and approximately 100 tonnes per year of dyes are discharged into waste streams [4]. The wastewater discharged from the textile industries are one of the major sources of wastewater production [5]. Methylene blue (MB) dye is the most commonly used basic dye for dyeing silk, cotton and wool [6]. The presence of dye containing water

can adversely affect the aquatic environment by impeding light penetration and precluding photosynthesis of aquatic flora [7]. Moreover, the toxic nature of the dye molecules route cause for several harmful effects such as allergy, dermatitis, skin irritation cancer, cell mutation, eye burns, gastritis, diarrhea, anemia, hypertension, vomiting, fever, and dizziness to the human beings and other living organisms [8]. Synthetic dyes are one kind of organic compound with a complex aromatic molecular structure that could provide bright and firm color to end products. However, the complex aromatic molecular structures of dyes make them more stable and difficult to biodegrade [9]. The researcher have been used several techniques such as electrochemical oxidation, ozonation, photocatalytic degradation, sonication, enzymatic treatment, adsorption, chemical coagulation, solvent extraction, bioremediation and photo catalytic degradation. However, these methods have a certain limitation,

\*Corresponding author.

such as low removal efficiency, high costs, and complex operation [10,11] and among all the techniques, adsorption was proved that most economical and efficient methods for the removal of noxious dyes from aqueous solution, it has been widely used to remove the dyes, because it is a simple and cost effective technique [12]. Today, many researchers have been used chitosan, bentonite, fly ash, peach kernel, olive, charcoal, barley, wheat, straw, sawdust [13], activated carbon, zeolites, carbon nanotubes, nanoparticles, nanocomposites, lignin, rubber tire and polymers as adsorbents [14]. Long and Young first reported that carbon nanotubes were more effective than activated carbon and other adsorbents for removing organic pollutants, these materials as new adsorbents attracted the attention of many researchers [15,16]. The porous carbon materials have attracted great attention in multidisciplinary areas due to their unique physical, chemical and mechanical properties [17]. The Carbon nanotubes (CNTs) have been intensively studied as a potential material to be used in various applications based on their remarkable physical and chemical properties [18]. Because of their easily modified surfaces and large surface areas, extensive experiments have been conducted for the adsorption of organic and inorganic pollutants on CNTs [19]. In last decade, the CNTs made a great interest for the treatment of organic and inorganic pollutants from the contaminated water [20]. The carbon materials functionalized with oxygen-containing groups on the surface of adsorbents have been used as a potential adsorbent for dye removal from aqueous solutions [21].

Nanofibrous technology is an advanced technique and has rapidly grown over the last decade for waste water treatment [22,23]. The non-woven material produced by the electrospinning technique [24] has fine diameter, large surface area, high porosity, high gas permeability and small pore size [25]. Recent researchers used 100% pure polymers (without copolymer) for preparation of nanofibres and few researchers have been used for dye removal, however the copolymers contains polyacrylonitrile (PAN) yarn waste have not been used as a adsorbent. Hence, in the present work, the polyacrylonitrile (PAN) textile yarn waste was used to prepare the nanofibrous adsorbent for dye removal.

Thus the present study has been focused on preparing polyacrylonitrile (PAN) Yarn waste/COOH-MCNT nanofibrous composite as adsorbent by electrospinning technique. The physical and chemical properties of the nanofibrous composites are studied using scanning electron microscope (SEM), X-ray diffractometer (XRD), Fourier transform infrared (FT-IR), and thermo gravimetric analyzer (TGA). The dye removal efficiency and adsorption capacity of the adsorbent have been studied using the UV-Vis spectrometer.

## 2. Materials and methods

The polyacrylonitrile polymer yarn waste was collected from textile industry. The carboxylic group functionalized multiwall carbon nanotube (COOH-MCNT) was dispersed in dimethyl formamide (DMF) and sonicated for 1 h. Polyacrylonitrile yarn waste was dissolved in the above solution followed by continuous magnetic stirring until homogeneous solution obtained. The solution was loaded into syringe fitted with needle. Then, the syringe was fixed

on syringe pump of the electrospinning unit. The distance between the needle and drum collector was set as 15 cm. The positive high voltage power supply anode was connected to the needle tip and negative voltage cathode was connected to aluminium drum collector. 15 kV was applied for the preparation of nanofibre. The flow rate of spinning solution was maintained as 1 mL/h. While applying 15 kV, the droplet of the polymer solution release from the tip of the needle break up and stretched to form the nanofibres. The fibres were collected on the rotating drum collector, simultaneously evaporation of solvent take place into atmosphere and remaining solvent evaporation under room temperature.

### 2.1. Adsorption experiment

The dye stock solution was prepared by dissolving 1 g methylene blue (sigma Aldrich) in 1000 mL of deionized water. The 10 ppm of working solution was made from the stock solution for all the experiments. Batch experiment was conducted for dye adsorption with adding 50 mg of nanofibrous composite into 100 mL of methylene blue dye solution (10 mg/L) under shaking condition at room temperature with optimized pH 10. The adsorption rate of the nanofibrous composite was studied at 10, 20, 30, and 40 mg/L dye concentration. The effect of pH, effect of contact time and the effect of COOH-MCNT dose on the dye adsorption rate of the nanofibrous composites were studied. The adsorption rate was measured as absorbance using the UV-Vis spectrometer (Hitachi U-2800, Japan), with a scanning range of 400–700 nm.

### 2.2. Characterization of Nanofibrous composite

The surface structure and shape of the polyacrylonitrile yarn waste/carboxylic group functionalized multi-walled carbon nanotube nanofibrous mat was studied by scanning electron microscopy. The average diameter of the nanofiber was measured from SEM image using Image Tool software (UTHSCSA). The FT-IR study was carried out to identify the characteristic functional groups present in the prepared nanofibrous composites at the wave number range of 400–4000  $\text{cm}^{-1}$ . The thermal stability of the nanofibrous composite was analyzed using TGA (Perkin-Elmer). The temperature scans ranged from C to C at /min under nitrogen gas atmosphere. The PAN yarn waste nanofiber and PAN yarn waste/multi-wall carbon nanotube nanofibrous composites were analysed by X-ray diffractometer, under using  $\text{CuK}\alpha$  ( $\lambda = 1.54$ ) radiation at 40Kv/200Ma. Scan was performed with 20 values ranging from 10 to 80° at a rate of 5°C/min.

## 3. Result and discussion

### 3.1. Scanning electron microscopic analysis

The surface morphology of polyacrylonitrile yarn waste/carboxylic group functionalized multi-wall carbon nanotube nanofibrous composite was analysed by using scanning electron microscope. The SEM image (Figs. 1a–d) shows the surface morphology of pristine PAN, PAN + 0.5 wt% COOH-MNCT, PAN + 1 wt% COOH-MCNT and

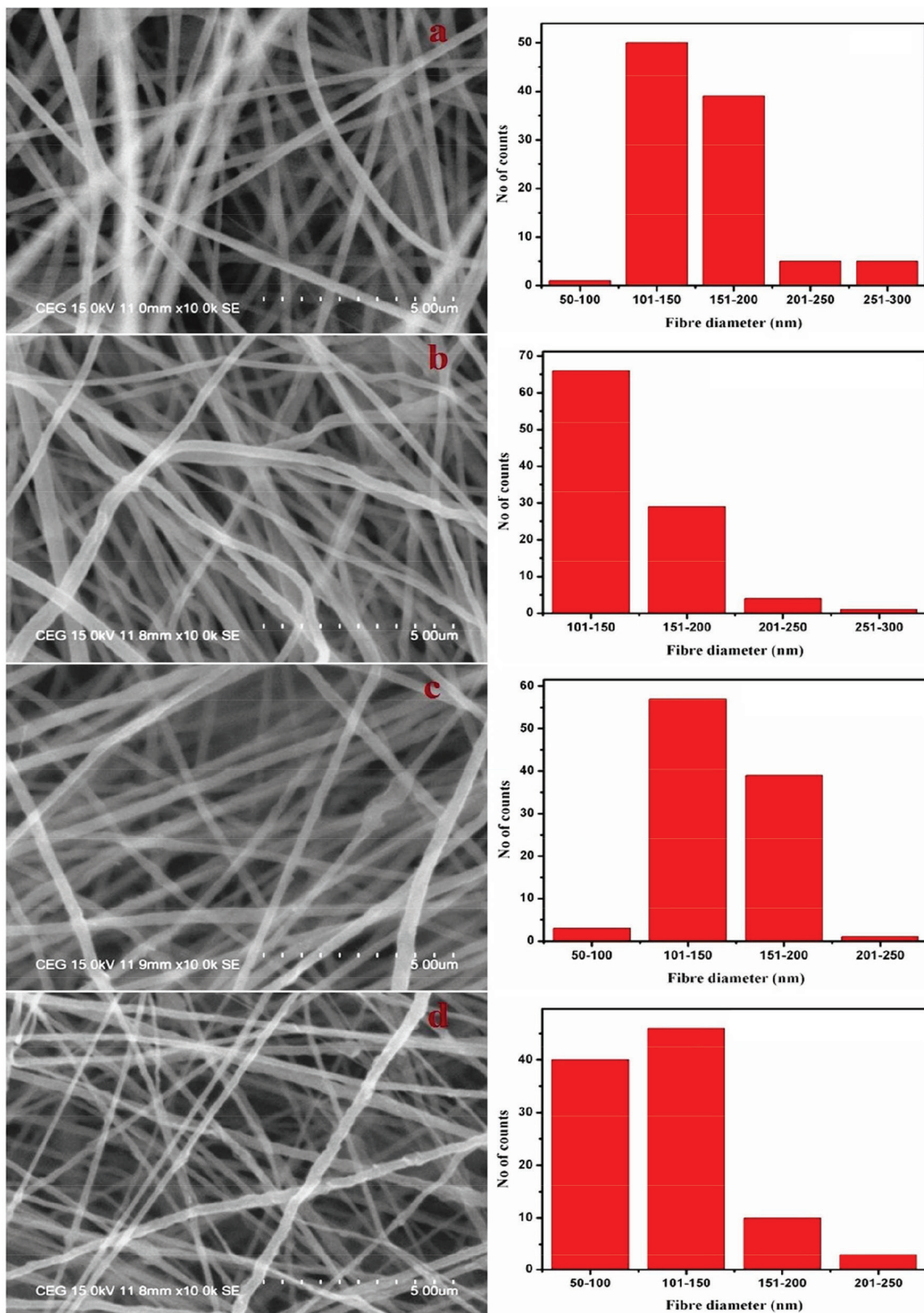


Fig. 1. SEM Images and distribution of fibre diameter (a) PAN (b) PAN + 0.5 wt% COOH-MCNT (c) PAN + 1 wt% COOH-MCNT (d) PAN + 1.5 wt% COOH-MCNT.

PAN + 1.5 wt% COOH-MCNT nanofibrous composites. From Figs. 1a–d it can be observed that the fiber diameter is decreased with an increasing the percentage of carboxylic group functionalized multi-wall carbon nanotube in the polymer solution, which may disturbed the alignment of crystalline region in the nanofibrous composite. It may be enhanced the performance of dye adsorption. The carbon nanotubes (CNTs) have the nano-scale diameter and tubular microstructure. The carbon nanotubes may be changed the smooth surface of nanofibrous composite to rough and irregular surface. The porous structure of carbon nanotubes also supported to improve the dye adsorption [26].

The percentage of C, N, and O elements were analyzed for pristine PAN yarn waste and PAN yarn waste/1.5 wt% COOH-MCNT using EDX. The percentage of C, N and O elements of pristine PAN yarn waste and PAN yarn waste/1.5 wt% COOH-MCNT nanofibrous composite is shown in Table 1. From Table 1 it is observed that the percentage of C and O was found to be higher in the PAN/1.5 wt% COOH-MCNT nanofibrous mat as compared with pristine PAN yarn waste nanofibrous mat. This may be due to the presence of carboxylic group in the PAN/1.5 wt% COOH-MCNT composite.

### 3.2. FT-IR analysis

FTIR spectra of the pristine PAN, PAN+0.5 wt% COOH-MCNT, PAN + 1 wt% COOH-MCNT and PAN + 1.5 wt% COOH-MCNT nanofibrous composites shown in Figs. 2a–d respectively. The vibrational band appeared between 2000–2500  $\text{cm}^{-1}$ , which may be assigned to the presence of the nitrile groups in the composite nanofibres [27]. The vibrational band is observed at 1452  $\text{cm}^{-1}$  due to the C-H bending of PAN. The spectra (Figs. 2b–d) show the sharp band at 1732  $\text{cm}^{-1}$  for PAN + 1 wt% COOH-MCNT and PAN + 1.5 wt% COOH-MCNT nanofibrous composites, due to the C=O stretching of functionalized multiwall carbon nanotube in the nanofibrous composites. From the result it could be observed that the sharp intensity band at 1732  $\text{cm}^{-1}$  in the PAN + 1.5 wt% COOH-MCNT nanofibrous mat. The intensity of vibration band at 1732  $\text{cm}^{-1}$  is increased with increasing the amount of COOH-MCNT. It may be confirmed the presence of COOH-MCNT in the nanofibrous composites.

### 3.3. X-Ray diffraction analysis

The XRD pattern (Figs. 3a–d) show for pristine PAN, PAN + 0.5 wt% COOH-MCNT, PAN + 1 wt% COOH-MCNT and PAN + 1.5 wt% COOH-MCNT respectively. The intensity peak is appeared at 16.9° (2 $\theta$ ) for all nanofibrous compos-

Table 1  
EDX analysis of PAN and PAN/COOH-MCNT nanofibrous composite

Atoms	PAN	PAN+COOH-MCNT
C%	19.31	20.75
N%	54.38	51.65
O%	26.30	27.60

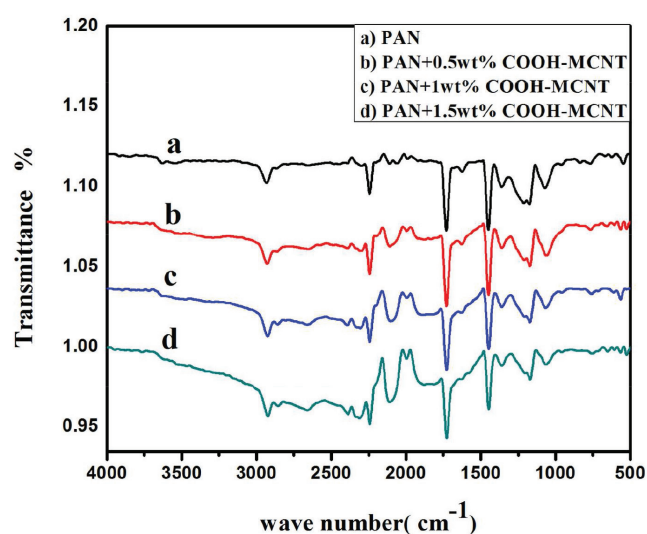


Fig. 2. FT-IR spectra of (a) PAN (b) PAN + 0.5 wt% COOH-MCNT (c) PAN + 1 wt% COOH-MCNT (d) PAN + 1.5 wt% COOH-MCNT.

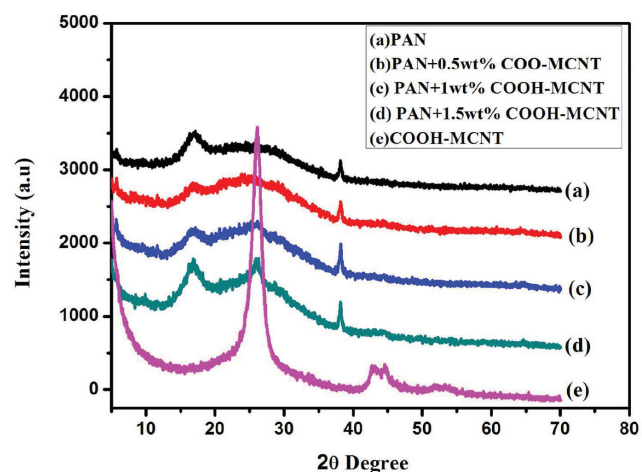


Fig. 3. XRD pattern of (a) PAN (b) PAN + 0.5 wt% COOH-MCNT (c) PAN + 1 wt% COOH-MCNT (d) PAN + 1.5 wt% COOH-MCNT.

ite mat with their corresponding space (d) of 5.24. The major intensity peak at 26.04° with the corresponding space of 3.14, which may be attributed the presence of COOH-MCNT in the nanofibrous composite. Whereas in Fig. 4b the peak at 26.04 (2 $\theta$ ) for COOH-MCNT not visible clearly, due to the lesser amount of COOH-MCNT distribution in the nanofibrous composite. From Fig. 3, the peak for COOH-MCNT is found to be very fine in the PAN + 1 wt% COOH-MCNT and PAN + 1.5 wt% COOH-MCNT nanofibrous composites.

### 3.4. Thermogravimetric analysis

The thermal stability of the pure PAN yarn waste and PAN Yarn waste/0.5, 1.0, 1.5 wt% COOH-MCNT nanofibrous composites were studied using TGA. Figs. 4a–d show the pristine PAN yarn waste and PAN yarn waste/0.5, 1.0, 1.5 wt% COOH-MCNT respectively. All nanofibrous mats show

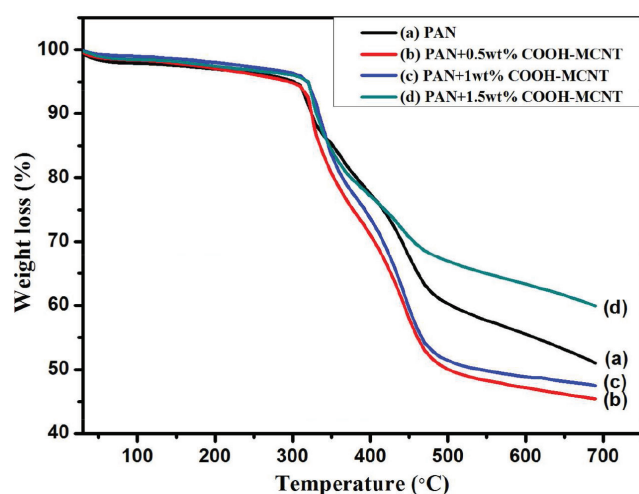


Fig. 4. Thermo gravimetric analysis of (a) PAN (b) PAN + 0.5 wt% COOH-MCNT (c) PAN + 1 wt% COOH-MCNT (d) PAN + 1.5 wt% COOH-MCNT.

the first weight loss at 100°C, which may be attributed to the evaporation of moisture in the nanofibrous mat. The second weight loss occurs at 210°C, due to the decomposition of backbone of the polymer chain. The third weight loss occurs at 310°C for pure PAN and 320°C for PAN/COOH-MCNT composites due to volatile components such as CO and CO<sub>2</sub>. From Fig. 4 it can be observed that the PAN/COOH-MCNT nanofibrous composites are showing higher thermal stability as compared with pristine PAN yarn waste nanofibrous mat.

### 3.5. Effect of initial pH

The pH of the solution is playing an important role in dye adsorption process. The adsorption capacity of the PAN yarn waste/COOH-MCNT nanofibrous composite was studied at different pH with 6 hrs fraction time. The effect of pH on adsorption of methylene blue was studied by varying the pH from 3 to 11 with fixed initial dye concentration of 10 mg/L and adsorbent dosage of 50 mg/L shown in Fig. 5. The adsorption capacity of the nanofibrous composite was increased when the pH of the solution increased from 3.0 to 11.0. Under acidic conditions adsorption capacity was significantly low. The maximum dye uptake capacity of 9.5 mg/g was obtained at pH 10. The dye adsorption rate was very low at lower pH and increased with increasing the pH of the solution. The maximum adsorption was found to be higher at basic pH. The pH of the dye solution may affect the surface charge of the adsorbent, the scale of ionization, functional groups on the active sites of the adsorbent as well as the structure of the dye molecule

### 3.6. Adsorption mechanism

The basic pH may enhance the anionic site on the PAN yarn waste/COOH-MCNT nanofibrous composite surface due to the presence of a higher number of active sites on the nanofibrous composite surface, which may be enhanced the dye adsorption by electrostatic interaction. At basic pH, the nitrile group of the PAN may be converted into carbox-

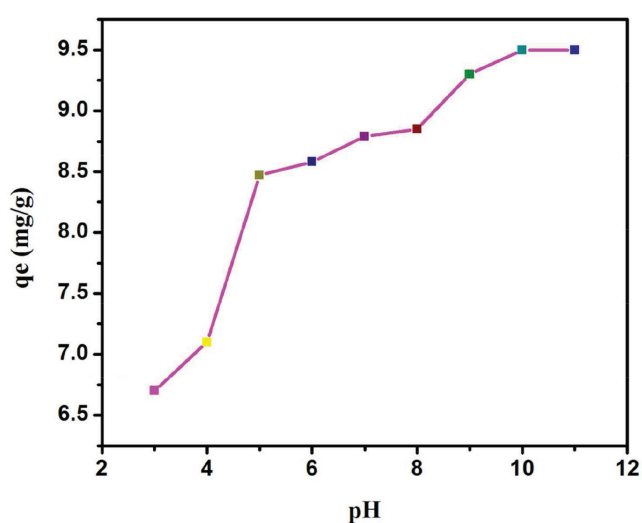


Fig. 5. Effect of pH on methylene blue adsorption.

ylic groups. The carboxylic groups in the composites are changed anionic site (COO<sup>-</sup>) under basic medium, which in turn to lead the electrostatic attraction between anionic surface of composite and cationic site of dye [28]

### 3.7. Effect of contact time and initial dye concentration

The dye adsorption capacity of the PAN yarn waste / COOH-MCNT nanofibrous composite was observed at different contact time intervals with an optimum pH 10. The dye uptake capacity was increased with increase in contact time. In the first phase, the dye adsorption rate of the PAN yarn waste /COOH-MCNT nanofibrous composite rapidly increased, which may be due to the outer surface's active sites with both physisorption and electrostatic chemisorptions, in the second stage gradual adsorption occurred, which may be in the inner active sites of the composite with fully chemisorption. Finally there is no significant colour change due to the saturation point. The PAN yarn waste/COOH-MCNT nanofibrous composite was studied with different dye concentration (10, 20, 30, and 40 mg/L) for 6 h at different time interval. From Fig. 6 it can be observed that the maximum dye up take is found at 30 mg/L of concentration.

### 3.8. Effect of COOH-MCNT dosage on dye removal

Fig. 7 shows the effect of COOH-MCNT dosage on dye removal. From the result, it could be observed that the dye removal efficiency increased with increase the percentage of COOH-MCNT. The maximum dye removal is found to be higher in the PAN yarn waste/1.5 wt% COOH-MCNT nanofibrous composite, than the pristine PAN yarn waste, PAN/0.5 wt% COOH-MCNT and PAN yarn waste/1.0 wt% COOH-MCNT. The COOH-MCNT enhanced the amorphous content in the polymer nanofibrous composite, due to dispersion of COOH-MCNT in the nanofibrous composite, and also it provided a rough surface to the nanofibrous composite. The rough surface and amorphous structure are factors that improve the dye removal efficiency [29].

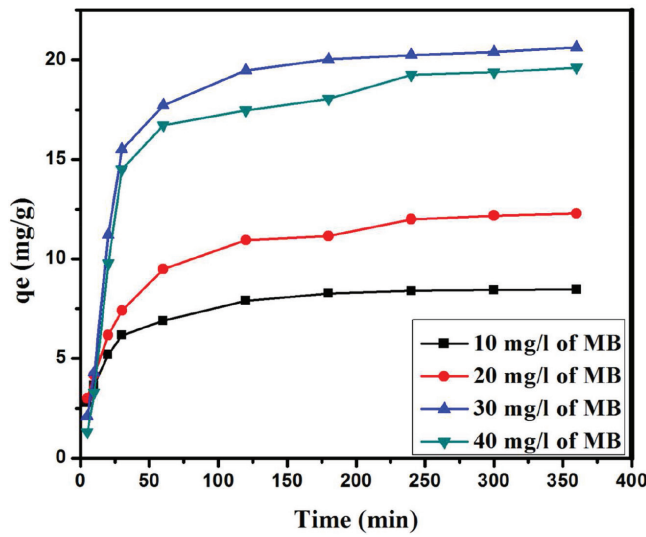


Fig. 6. Effect of contact time with initial dye concentration on adsorption.

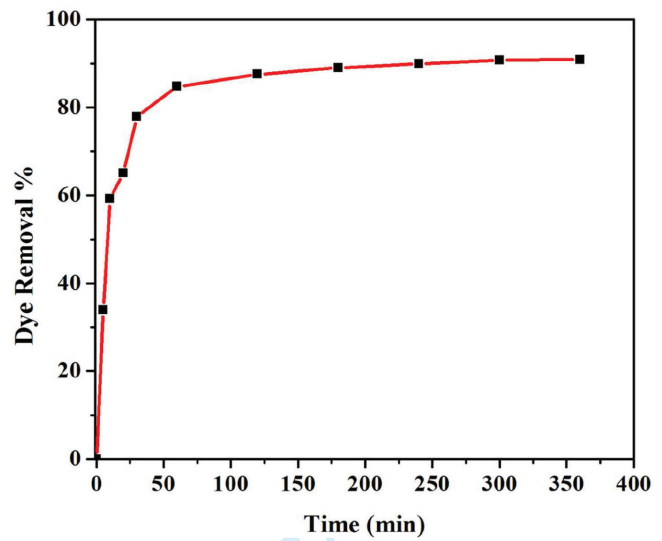


Fig. 8. Dye Removal efficiency with contact time.

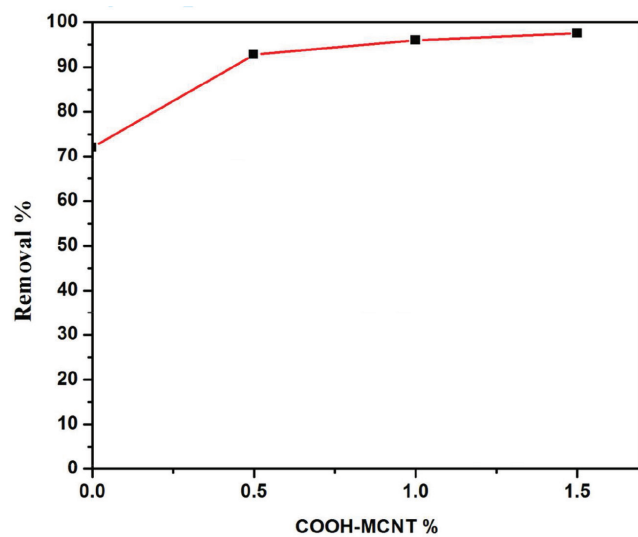


Fig. 7. Effect of COOH-MCNT dosage on methylene blue adsorption.

### 3.9. Dye removal efficiency

The fast dye removal rate was occurred in the first 60 min as shown in Fig. 8, due to the presence of more outer surface active sites on the nanofibrous composite. Then gradually increased up to a certain period of contact time, which may be due to the inner surface phenomenon. The system may reached the saturation point, after blocking the all pores and active sites in the nanofibrous composite.

### 3.10. Adsorption kinetics

A kinetic study is playing an important role to predict the appropriate rate of adsorption of methylene blue on the

absorbent. The kinetics of adsorption showed the dye uptake rate and also gives the residence time of the adsorption. The rate controlling steps and diffusion mechanism have been studied using the pseudo-first order, pseudo-second order kinetics and external diffusion models respectively. Pseudo-first order kinetic equation is given as Eq. (1) [30].

$$\ln(q_e - q_t) = \ln q_e - k'_t t \quad (1)$$

The slope and intercept of  $\ln(q_e - q_t)$  vs. time (Fig. 9a) yield, the values of  $k'_t$ , and the predicted  $q_e$  and experimental  $q_e$  values obtained for the adsorption of methylene blue dye solution on the PAN yarn waste/COOH-MCNT nanofibrous composite. In pseudo-second order model, it is assumed that the adsorption capacity is proportional to the number of active sites present in the absorbent, and then the kinetic rate equation is given as Eq. (2) [31,32].

$$\frac{t}{q_t} = \frac{1}{h} + t \left( \frac{1}{q_e} \right) \quad (2)$$

where  $h = k'_2 * q_e^2$ . The values  $(1/h)$  and  $q_e$  can be determined from the intercept and slope, respectively, from a linear plot of  $t/q_t$  vs. time (Fig. 9b).

The external diffusion model is given by Eq. (3) [33].

$$\ln \frac{C_t}{C_0} = -k_{ext} t \quad (3)$$

The plot of  $\ln(C_t)$  vs. time (Fig. 9c) gives a linear relationship for external diffusion model. From Table 2, the  $R^2$  value is found to be higher in the second order than the first order. From the result, it could be observed that the Pseudo-second order kinetic model most fitted for the adsorption of methylene blue dye while compared to other models.

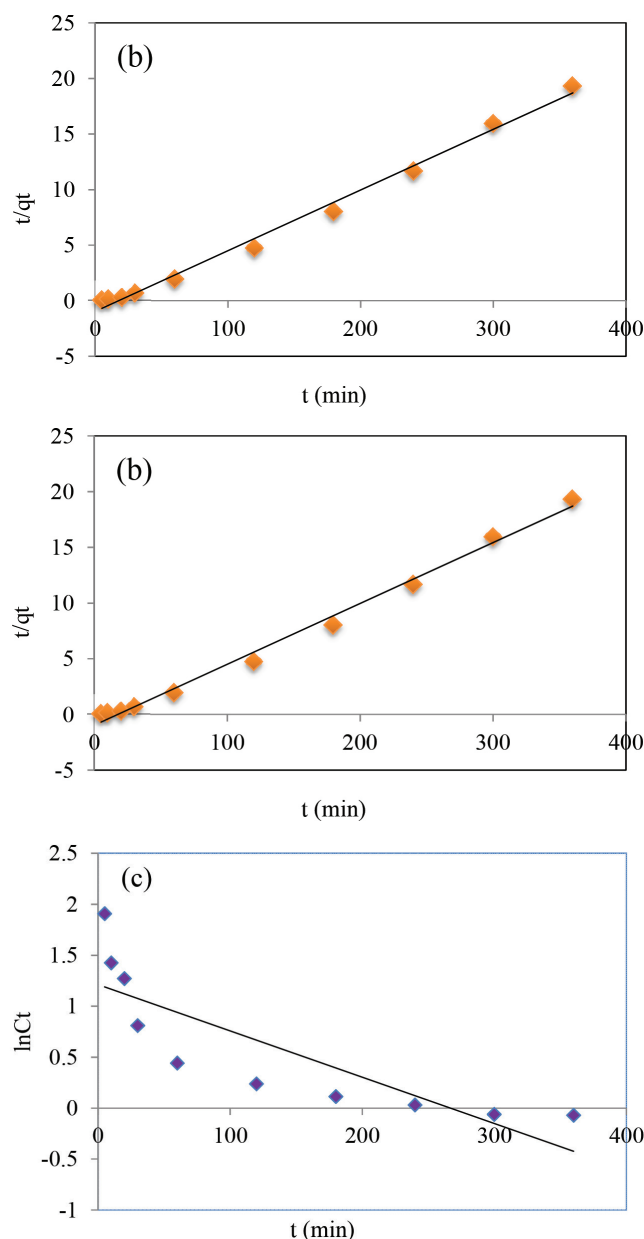


Fig. 9. (a) Pseudo-first order kinetic model, (b) Pseudo-second order kinetic model, and (c) External diffusion model.

### 3.11. Adsorption isotherms

The adsorption isotherm determines molecular attraction between the liquid phase and the solid phase when the adsorption process is reached at equilibrium level. The adsorption isotherm model is playing an important role to know the adsorptive behaviour of solid-liquid adsorption systems. To optimize the adsorbent's usage, the adsorption isotherm is used to find how solutes interact with adsorbents. The three isotherm models are used to study the adsorptive behaviour of nanofibrous composite namely, Langmuir, Freundlich and Scatchard adsorption isotherms. The applicability of these three isotherms was compared by

Table 2  
Kinetic constants for the adsorption equilibrium of methylene blue on Polyacrylonitrile yarn waste /COOH-MCNT nanofibrous composite

Kinetic model	Methylene Blue
Pseudo first order	
$k'_1$ (min <sup>-1</sup> )	0.0064
$R^2$	0.7697
Pseudo second order	
$k'_2$ (g/(mg min))	0.0031
$R^2$	0.9928
$h$ (mg/(g min))	1.0349
$q_{cal}$ (mg/g)	18.2815
External diffusion model	
$k_{ext}$ (l/min)	0.0045
$R^2$	0.7043

evaluating the correlation coefficients. Langmuir isotherm is given as

$$\frac{c_e}{q_e} = \frac{1}{bQ_0} + \frac{1}{Q_0} c_e \quad (4)$$

where  $C_e$  is the equilibrium concentration of the dye solution (mg L<sup>-1</sup>),  $q_e$  is the amount of dye adsorbate per unit mass of adsorbent (mg/g). The Langmuir parameters  $Q_0$  (mg/g) and  $b$  (L/mg) indicate the maximum adsorption capacity and the rate of adsorption, respectively. The  $Q_0$  and  $b$  are obtained from the slope and intercept of the straight lines of plot  $C_e/q_e$  vs.  $C_e$  (Fig. 10a).

The shape of Langmuir isotherm could also be expressed in terms of adsorption factor ( $R_L$ ), which is given as follows.

$$R_L = \frac{1}{1 + bC_0} \quad (5)$$

where  $b$  is Langmuir constant (L/mg) which related to the affinity of binding sites and the energy of adsorption and  $C_0$  is initial concentration of dye. The  $R_L$  and  $R^2$  parameters are obtained from the Langmuir isotherm model which is given in table. If the ( $R_L$ ) is unfavourable, ( $R_L = 1$ ) linear, ( $0 < R_L < 1$ ) favourable, and ( $R_L = 0$ ) irreversible [34].

The Table 3 shows the  $R_L$  value in the range between 0 and 1, from which it could be favourable for the adsorption of methylene blue.

The Freundlich isotherm illustrates the heterogeneity of the adsorbent surface involving a multilayer adsorption. The Freundlich equation was used for the adsorption of Methylene blue on the adsorbent. The Freundlich isotherm was represented as

$$\ln q_e = \ln k_f + \frac{1}{n} \ln c_e \quad (6)$$

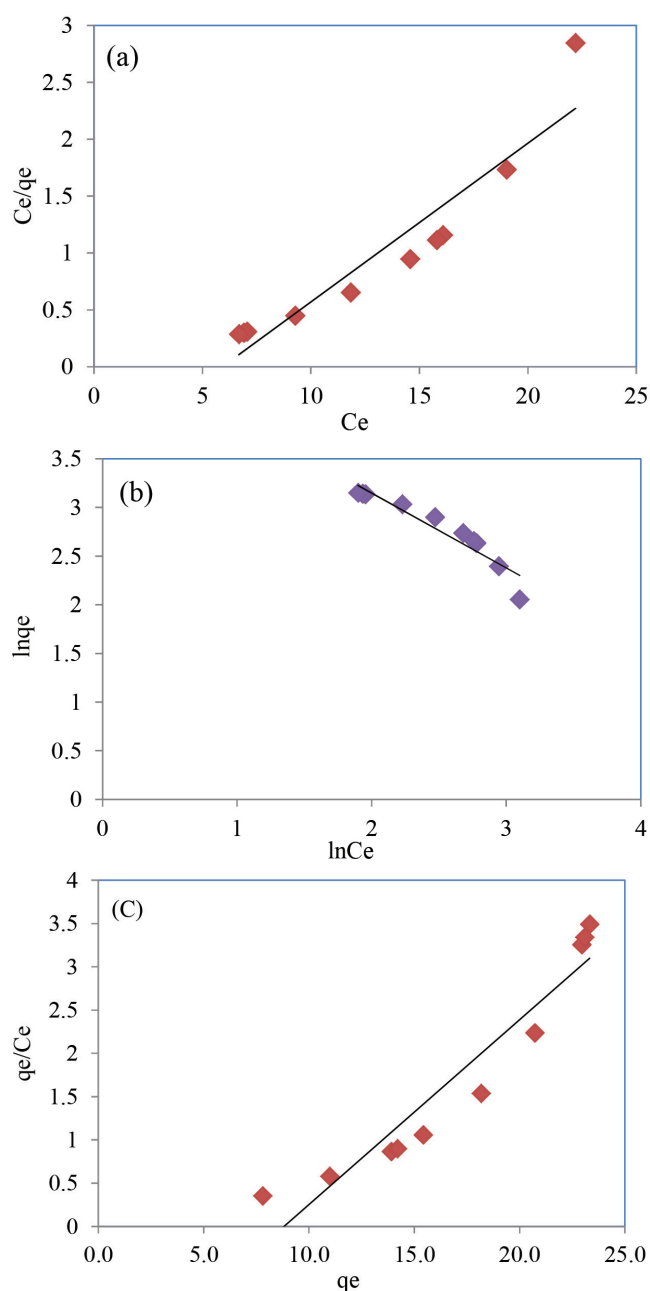


Fig. 10. (a) Langmuir isotherm model, (b) Freundlich isotherm model, and (c) Scatchard isotherm model.

where the parameters  $K_f$  and  $1/n$  indicated the sorption capacity and the sorption intensity of the system respectively. The  $K_f$  and  $1/n$  values are presented in Table 2. The  $K_f$  and  $1/n$  are obtained from the slope and intercept of the straight lines of plot  $\ln q_e$  vs.  $\ln C_e$  (Fig. 10b). Generally the  $1/n$  value is occurring between 0 and 1 for favourable adsorption of adsorbate on adsorbent [35]. The  $1/n$  values obtained from Freundlich isotherm model is 0.7716, which is occurring in the range of 0–1. From the result it could be concluded that the adsorbent is more favourable for methylene blue adsorption.

Table 3

Isotherm constants for the adsorption of methylene blue on Polyacrylonitrile yarn waste/COOH-MCNT nanofibrous composite at room temperature

Isotherm	Constants
Langmuir	
$Q_o$ , mg/g	7.1685
$b$ , L/mg	0.1687
$R^2$	0.8881
$R_L$	0.1650
Freundlich	
$1/n$	0.7716
$k_f$ (L/mg)	1.5459
$R^2$	0.9007
Scatchard	
$q_m$ (mg/g)	8.81
$K_L$ (L/mg)	0.2137
$R^2$	0.9122

The Scatchard isotherm model is used to study the binding sites of adsorbent, the Scatchard equation can be written as

$$\frac{q_e}{c_e} = q_m K_L - q_e K_L \quad (7)$$

where  $q_e$  and  $C_e$  are the equilibrium adsorption capacity of the adsorbent and the equilibrium concentration of adsorbate respectively. The parameters  $q_m$  and  $K_L$  are represents the number of binding sites and affinity of the adsorbent respectively. The  $q_m$  and  $K_L$  are obtained from the slope and intercept of the straight line plot of  $q_e/C_e$  vs.  $C_e$  (Fig. 10c). The  $R^2$  and  $K_L$  values are obtained from the Scatchard isotherm model. The Scatchard plot is showing down curvature line for methylene blue adsorption. The down curvature line suggests that the successive adsorbate molecules are bound more strongly on adsorbent [36]. From the result it could be observed that the Freundlich and Scatchard isotherm models are more favourable for the adsorption of methylene blue than Langmuir model.

#### 4. Conclusions

The prepared PAN nanofibrous composite was a potential adsorbent for the removal of methylene blue dye. The nanofibrous composite was acquired the maximum amount of methylene blue dye removal under basic pH. The percentage of dye removal was found to be higher in the PAN/1.5 wt% COOH-MCNT composite as compared with other composites. The  $R^2$  value was found to be higher in the Freundlich and scatchard isotherm models. It shows the enhanced multilayer adsorption of nanofibrous composite. Freundlich and scatchard isotherm models were indicated the number of adsorption layer and active binding sites in the adsorbent respectively. The pseudo second order kinetic model was



found to be most fit for the adsorption of methylene blue. The maximum of 77.74% dye removal was attained by using prepared PAN yarn waste/COOH-MCNT nanofibrous composite for 30 initial dye concentrations.

### Acknowledgement

The authors would like to thank the University Grand Commission, New Delhi, India for providing the funding facility to carry out this research work. UGC Sanction No. F.7-288/2009 (BSR), dated 27.12.2013.

The authors are thankful to Dr. R. Jayavel and Mr. M. Shanmugam, Centre for Nanoscience and Technology, Anna University, Chennai, India for providing an instrumental facility.

### Symbols

$Q_{ov}$	$b$	—	Langmuir isotherm constant (l/mg)
$C_o$		—	Initial liquid-phase concentration (mg/L)
$C_e$		—	Equilibrium liquid-phase concentration (mg/L)
$K_f$		—	Freundlich isotherm constant (L/mg)
$K_L$		—	Scatchard isotherm constant (L/mg)
$N$		—	Freundlich isotherm constant
$q_e$		—	Equilibrium uptake capacity (mg/g)
$K'_1$		—	Pseudo first order rate constant ( $\text{min}^{-1}$ )
$K'_2$		—	Pseudo second order rate constant (g/mg min)
$K_{ext}$		—	External diffusion constant (min)
$R_L$		—	Dimensionless constant separation factor

### References

- [1] W.S. Alencar, E.C. Lima, B. Royer, B.D. Dos Santos, T. Calvete, E.A. Da Silva, C.N. Alves, Application of Aqai stalks as biosorbents for the removal of the dye Procion Blue MX-R from aqueous solution, *Sep. Sci. Technol.*, 47 (2012) 513–526.
- [2] C.I. Pearce, J.R. Lloyd, J.T. Guthrie, The removal of color from textile wastewater using whole bacterial cells: A review, *Dyes Pigm.*, 58 (2003) 179–196.
- [3] G. McMullan, C. Meehan, A. Conneely, N. Kirby, T. Robinson, P. Nigam, I.M. Banat, R. Marchant, W.F. Smyth, Microbial decolorization and degradation of textile dyes, *Appl. Microbiol. Biotechnol.*, 56 (2001) 81–87.
- [4] N. Dizge, C. Aydinler, E. Demirbas, M. Kobya, S. Kara, Adsorption of reactive dyes from aqueous solutions by fly ash: kinetic and equilibrium studies, *J. Hazard. Mater.*, 150 (2008) 737–746.
- [5] P. Senthil Kumar, J. Pavithra, S. Suriya, M. Ramesh, K. Anish Kumar, Sargassum wightii, a marine alga is the source for the production of algal oil, bio-oil, and application in the dye wastewater treatment, *Desal. Water Treat.*, 55 (2015) 1342–1358.
- [6] P. Senthil Kumar, R. Sivaranjane, U. Vinothini, M. Raghavi, K. Rajasekar, K. Ramakrishnan, Adsorption of dye onto raw and surface modified tamarind seeds: Isotherms, process design, kinetics and mechanism, *Desal. Water Treat.*, 52 (2014) 2620–2633.
- [7] N.F. Cardoso, E.C. Lima, I.S. Pinto, C.V. Amavisca, B. Royer, R.B. Pinto, W.S. Alencar, S.F.P. Pereira, Application of cupuassu shell as biosorbent for the removal of textile dyes from aqueous solution, *J. Environ. Manage.*, 92 (2011) 1237–1247.
- [8] R.O. Alves de Lima, A.P. Bazo, D.M. Salvadori, C.M. Rech, D. De Palma Oliveira, G. De Aragão Umbuzeiro, Mutagenic and carcinogenic potential of a textile azo dye processing plant effluent that impacts a drinking water source, *Mutat. Res. Genet. Toxicol. Environ. Mutagen.*, 626 (2007) 53–60.
- [9] L.D. Prola, F.M. Machado, C.P. Bergmann, F.E. De Souza, C.R. Gally, E.C. Lima, M.A. Adebayo, S.L. Dias, T. Calvete, Adsorption of Direct Blue 53 dye from aqueous solutions by multi-walled carbon nanotubes and activated carbon, *J. Environ. Manage.*, 130 (2013) 166–175.
- [10] F. Gholami Borujeni, A.H. Mahvi, S. Naseri, M.A. Faramarzi, R.R. Nabizadeh, M.A. Mohammadi, Enzymatic treatment and detoxification of Acid Orange 7 from textile wastewater, *App. Biochem. Biotechnol.*, 165 (2011) 1274–1284.
- [11] V. Mathivanan, S. Geetha Manjari, R. Ineya, R. Saravanathamizhan, P. Senthil Kumar, K. Ramakrishnan, Enhanced photocatalytic decolorization of reactive red by sonocatalysis using TiO<sub>2</sub> catalyst: Factorial design of experiments, *Desal. Water Treat.*, 57 (2016) 7120–7129.
- [12] V.K. Gupta, S. Agarwal, T.A. Saleh, Chromium removal by combining the magnetic properties of iron oxide with adsorption properties of carbon nanotubes, *Water Res.*, 45 (2011) 2207–2212.
- [13] S. Dazhong, J. Fana, Z. Weizhi, G. Baoyu, Y. Qin Yan, Q. Kanga, Adsorption kinetics and isotherm of anionic dyes onto organo-bentonite from single and multisolute systems, *J. Hazard. Mater.*, 172 (2009) 99–107.
- [14] H. Sadegh, R. Ghoshekandi, S. Agarwal, I. Tyagi, M. Asif, V.K. Gupta, Microwave-assisted removal of malachite green by carboxylate functionalized multi-walled carbon nanotubes: Kinetics and equilibrium study, *J. Molec. Liq.*, 206 (2015) 151–158.
- [15] R. Long, R. Yang, Carbon nanotubes as superior sorbent for dioxin removal, *J. Am. Chem. Soc.*, 123(9) (2001) 2058–2059.
- [16] W. Konicki, I. Petech, E. Mijowska, I.J. Ska, Adsorption of anionic dye Direct Red 23 onto magnetic multi-walled carbon nanotubes-Fe<sub>3</sub>C nanocomposite: Kinetics, equilibrium and thermodynamics, *Chem. Eng. J.*, 210 (2012) 87–95.
- [17] S.B. Fagan, A.G.S. Filho, J.O.G. Lima, J.M. Filho, O.P. Ferreira, I.O. Mazali et al., 1,2-Dichlorobenzene interacting with carbon nanotubes, *Nano Lett.*, 4(7) (2004) 1285–1288.
- [18] G.P. Rao, C. Lu, F. Su, Sorption of divalent metal ions from aqueous solution by carbon nanotubes: A review, *Sep. Purif. Technol.*, 58 (2007) 24–231.
- [19] V.K. Gupta, B. Gupta, A. Rastogi, S. Agarwal, A. Nayak, A comparative investigation on adsorption performances of mesoporous activated carbon prepared from waste rubber tire and activated carbon for a hazardous azo dye-Acid Blue 113, *J. Hazard. Mater.*, 186 (2011) 891–901.
- [20] T.A. Saleh, V.K. Gupta, Column with CNT/magnesium oxide composite for lead (II) removal from water, *Environ. Sci. Pollut. Res.*, 19 (2012) 1224–1228.
- [21] L. Ai, L. Li, Efficient removal of organic dyes from aqueous solution with ecofriendly biomass-derived carbon@montmorillonite nanocomposites by one-step hydrothermal process, *Chem. Eng. J.*, 223 (2013) 688–695.
- [22] W.E. Teo, S. Ramakrishna, A review on electrospinning design and nanofiber assemblies, *Nanotechnology*, 17 (2006) 89–106.
- [23] K. Ohkawa, D. Cha, H. Kim, A. Nishida, H. Yamamoto, Electrospinning of chitosan, *Macromol. Rapid Commun.*, 25 (2004) 1600–1605.
- [24] C.J. Buchko, L.C. Chena, Y. Shena, D.C. Martin, Processing and microstructural characterization of porous biocompatible protein polymer thin films, *Polymer*, 40 (1999) 7397–7407.
- [25] W. Qingqing, D. Yuanzhi, F. Quan, H. Fenglin, L. Keyu, L. Jingyan, W. Qufu, Nanostructures and surface nanomechanical properties of polyacrylonitrile/graphene oxide composite nanofibers by electrospinning, *J. Appl. Polym. Sci.*, 128 (2013) 1152–1157.
- [26] X. Li, C. Zeng, J. Jiang, L. Ai, Magnetic cobalt nanoparticles embedded in hierarchically porous nitrogen-doped carbon frameworks for highly efficient and well-recyclable catalysis, *J. Mater. Chem. A.*, 4 (2016) 7476–7482.
- [27] K. Saeed, S. Haider, T.J. Oh, S.Y. Park, Preparation of amidoxime modified polyacrylonitrile (PAN-oxime) nanofibers and their applications to metal ions adsorption, *J. Membr. Sci.*, 322 (2008) 400–405.
- [28] S. Saber-Samandari, H. Joneidi-Yekta, M. Mohseni, Adsorption of anionic and cationic dyes from aqueous solution using gela-

- tin-based magnetic nanocomposite beads comprising carboxylic acid functionalized carbon nanotube, Chem. Eng. J., 308 (2017) 1133–1144.
- [29] S. Swaminathan, A. Muthumanickam, N.M. Imayathamizhan, An effective Removal of Methylene blue dye using Polyacrylonitrile Yarn waste/ Graphene oxide nanofibrous composite, Int. J. Environ. Sci. Technol., 12 (2015) 3499–3508.
- [30] S. Lagergren, B.K. Svenska, Zur theorie der sogenannten adsorption gelöster stoffe, Vetenskaps Akad, Handl., 24 (1898) 1–39.
- [31] Y.S. Ho, G. McKay, Pseudo-second order model for sorption processes, Process Biochem., 34 (1999) 451–465.
- [32] G. Baskar, S.K. Pavithraa, K. Sheraz Fahada, S. Renganathan, Optimization, equilibrium, kinetic modeling, and thermodynamic studies of biosorption of aniline blue by the dead biomass of *Aspergillus fumigates*, Desal. Water Treat., 52 (2014) 3547–3554.
- [33] K.R. Hall, L.C. Eagleton, A. Acrivers, T. Vermenlem, Pore and solid diffusion and kinetics in fixed adsorption constant pattern conditions, Ind. Eng. Chem. Res., 5 (1966) 212–223.
- [34] M. Khan, I.M. Lo, Removal of ionizable aromatic pollutants from contaminated water using nano -Fe<sub>2</sub>O<sub>3</sub> based magnetic cationic hydrogel: Sorptive performance, magnetic separation and reusability, J. Hazard. Mater., 322 (2017) 195–204.
- [35] D.M. Manohar, B.F. Noeline, T.S. Anirudhan, Adsorption performance of Al-pillared bentonite clay for the removal of cobalt (II) from aqueous phase, Appl. Clay Sci., 31 (2006) 194–206.
- [36] C.H. Liu, J.S. Wu, H.C. Chiu, S.Y. Suen, K.H. Chu, Removal of anionic reactive dyes from water using anion exchange membranes as adsorbers, Water Res., 41 (2007) 1491–1500.